A&A manuscript no.
(will be inserted by hand later)

Your thesaurus codes are:
09.09.1 09.04.1 09.03.1 13.09.3

ASTRONOMY
AND
ASTROPHYSICS
4.11.1996

Letter to the editor: first results from ISO

ISOCAM mapping of the ρ Ophiuchi main cloud

A. Abergel[1], J.P. Bernard[1], F. Boulanger[1], C. Cesarsky[4], F.X. Désert[1], E. Falgarone[2], G. Lagache[1], M. Perault[2], J.–L. Puget[1], W.T. Reach[1], L. Nordh[3], G. Olofsson[3], M. Huldtgren[3], A.A. Kaas[3], P. André[4], S. Bontemps[34], M. Burgdorf[5], E. Copet[6], J. Davies[7], T. Montmerle[4], P. Persi[8], F. Sibille[9]

[1] Institut d'Astrophysique Spatiale, Université Paris-Sud, Bât.121, F-91405, Orsay, France
[2] Radioastronomie Millimétrique, Ecole Normale Supérieure, 24 rue Lhomond - 75005 Paris - France
[3] Stockholm Observatory, S-133 36 Saltsjöbaden, Sweden
[4] Service d'Astrophysique, Centre d'Etudes de Saclay, F-91191 Gif-Sur-Yvette Cedex, France
[5] ISO, Villafranco del Castillo, ESA Satellie tracking station, POB 50727, 28080 Madrid, Spain
[6] DESPA, Observatoire de Paris-Meudon, 5 place Jules Janssen, 92195 Meudon Cedex, France
[7] Joint Astronomy Center, 660 N. A'Ohoku Place, University Park, Hilo, HI 96720, USA
[8] Instituto Astrofisica Spaziale, CNR, v. E. Fermi 21, 00044 Frascati, Italy
[9] Observatoire de Lyon, 69230 Saint Genis Laval, France

Received date: July 16, 1996; accepted date: September 1, 1996

Abstract. We present preliminary results of the ISOCAM survey of the ρ Ophiuchi main cloud L1688 (0.5 square degrees) conducted in the two broad-band filters LW2 (5-8.5 μm) and LW3 (12-18 μm). This letter focuses on the properties of the extended emission. ISOCAM observations have revealed several previously unknown characteristics of the mid–IR diffuse emission: the small scale filamentary structure (thickness ~ 0.03 pc) of the emission at the illuminated edge of the molecular cloud, the sharpness of color variations at cloud edges, the barely resolved filamentary structure of the dust emission surrounding a bright embedded source, and several dense cores seen as sharp and deep absorption structures against the diffuse cloud background.

Key words: – ISM: individual objects: ρ Ophiuchus – ISM: dust, extinction – ISM: clouds – Infrared: ISM: clouds

1. Introduction

The observations described in this letter are part of the ISO central program dedicated to the survey of nearby star forming regions. The ρ Oph region is one of the nearest (160 pc, Bertiau 1958) extended molecular complex located at high galactic latitude (b$\simeq$17°). The main cloud (L1688) is totally opaque on optical plates and harbors some of the brightest spots of the Solar Neighborhood in the ^{12}CO, ^{13}CO and C^{18}O lines (Encrenaz et al. 1975, Wilking & Lada 1983, Loren 1989). The molecular complex is heated on large scales by the nearby Sco OB2 association (de Geus et al. 1989). Young embedded B stars have been detected via their associated compact HII regions (Brown & Zuckerman 1975, Falgarone & Gilmore 1981, André et al. 1992 and references therein). A large number of associated Young Stellar Objects (YSOs) have been indentified in L1688: 78 from (Wilking et al. 1989) and 332 from a J, H and K survey (Greene & Young 1992). The unusually high IR brightness of L1688 is due to large column densities (A$_v$ up to 100) combined with the presence of early type stars and YSOs. In this Letter, we concentrate solely on the analysis of this diffuse emission.

The large amount of work done on the diffuse emission in the IRAS images illustrate how useful this emission is to study the spatial structure of clouds, the interaction of young stars with nearby dense gas and the evolution of dust within the interstellar medium. An important result is the variations of the colors of the IR emission (e.g. Boulanger et al. 1990) which imply local changes in the abundance of small dust particles. In particular a striking 12 μm limb–brightening effect was discovered at the edge of the ρ Oph main cloud (Bernard et al. 1993). The much better angular resolution and sensitivity of the ISOCAM instrument (Cesarsky et al. 1996) greatly increases our ability to describe the structure of dense gas illumi-

Send offprint requests to: A. Abergel

nated by nearby bright stars, in particular the small scale variations in dust composition.

2. Observation strategy and data reduction

The L1688 cloud has been mapped using the LW2 (5-8.5 μm) and LW3 (12-18 μm) filters of ISOCAM, centered to 6.75 and 15 μm respectively. A $0.75° \times 0.75°$ square has been covered by six different rasters, with a scanning direction parallel to the equatorial direction, with $\Delta\alpha$ and $\Delta\delta$ equal to 0.6 and 0.8 times the frame size respectively. The 6" pixel-field-of-view lens was used for 4 rasters, and the 3" lens for the raster around the Source 1 (the brightest IR source of the field) and in the southern region to avoid saturation and detect structures with a better angular resolution. At each raster position, 60 frames were taken with the minimal integration time (0.28 s). The slew time between 2 successive positions is ~5 s. The whole field has been covered using 1104 sky positions. Per filter, the total number of transmitted frames is ~84000, and the total observing time ~23520 s.

Each raster has been reduced independently. First cosmic rays events are discarded using temporal median filtering (typically 4% of the data), then an averaged dark image obtained during the Performance Verification (PV) phase of ISO is subtracted from all frames. The accuracy of the dark subtraction is ~0.3 ADU (Digital Units). The smallest observed brightnesses are 18 and 70 ADUs in the LW2 and LW3 filters respectively, so the dark correction uncertainty is less than 3% in the two filters.

The LW array presents a time lagged response after a flux step. Typically the time constants for small steps above the zodiacal foreground at these wavelengths can be as high as several hundred readouts. If no correction for transient effects is applied, the fluxes are thus underestimated (resp. overestimated) for increasing (resp. decreasing) fluxes as function of time, and the computed images appear strongly degraded by trails along the scanning direction. We have developed a first order mathemathical model of the LW array response, where the measured signal at time t, $M(t)$, depends on the input flux I following the formula:

$$M(t) = rI(t) + (1-r)\int_{-\infty}^{t} dt' I(t') \frac{e^{-\frac{t-t'}{\tau(t')}}}{\tau(t')} \qquad (1)$$

where r corresponds to the instantanous response, and $\tau(t') = \alpha/M(t')$. ¿From preliminary fitting of our model with the transient responses recorded during the PV phase, we have obtained r = 0.6 and α= 1200 s/ADU. This model can be easily inverted, and $I(t)$ is computed using the successive values of $M(t)$. This is an experimental algorithm which will need improvements in the future. After correction, the memory effect is no longer visible after a few readouts (typically 1-3) for small flux steps (up or down), and the photometry is corrected. However this preliminary algorithm fails for strong steps, especially for the bright point sources visible on Fig. 1 where a systematic undershoot is still visible after correction. Note also that cosmic rays with memory effects can be mistaken for point sources. Therefore no discussion of the low mass YSOs will be given here, due to the preliminary status of the data reduction.

After the correction for transient effects, all the frames were coadded for each sky position. One flat field was extracted from each raster by computing the mean value of the lowest percentile (20%) seen by each pixel, excluding frames with strong emission above the zodiacal background. It is a first order estimate, since the large scale gradients of the sky brightness contaminate the computed flat field image. The optimisation of the flat field correction is still in progress. Finally coadded images are projected on the sky map. The ADU to MJysr^{-1} conversion is made using ISOCAM user's manual tables based on pre-launch photometry without any color correction.

Computed at the time of ISOCAM observations, the model of Reach et al. (1995), calibrated from DIRBE experiment data on board the COBE satellite, gives a zodiacal emission equal to 5.7$\pm$1 and 45$\pm$9 MJysr^{-1} at 6.75 μm and 15 μm respectively ($\beta \simeq$-2.5°), without any spatial variation within the field larger than a few %. These values are comparable to the minimal brightnesses of our maps (near the bottom left corner of Fig. 1): $I_\nu(6.75\mu m)$ = 8.6 and $I_\nu(15\mu m)$ = 39 MJysr^{-1}. We therefore adopt a foreground emission equal to 5.7$\pm$1 and 39^{+0}_{-3}MJysr^{-1} respectively.

3. Results and discussion

The structure of the extended emission in the ISOCAM maps (see Fig.1, or for more details the image on the ESTEC ISO WWW Server, where the emissions at 6.75 and 15 μm are coded in blue and red respectively) results from the interaction of young stars with the dense gas and the presence of very opaque condensations.

3.1. Interaction between young stars and dense gas

The analysis of the large scale IRAS emission of the ρ Oph complex has shown that the L1688 cloud edges are heated to the North by the two B2IV–V stars ρ Oph A and B and to the West by the B2V star HD147889 (α_{2000}=16h 25m 24.2s, δ_{2000}=-24°27'55"), just out of the field. The dust heated by these stars is responsible for the large 100 μm brightness of this cloud (Bernard et al. 1993). The ISOCAM map is centered on the dense cloud and includes only a small part of the Northern edge. We believe the dust heated mostly by the star HD147889 emits the extended emission to the West of the map. The bright filaments in the region around $\alpha_{2000} \sim$ 16h 26m, $\delta_{2000} \sim$ -24°22' have a remarkable spatial coherence, and closely follow the western edge of the 1 $\times$2 pc $C^{18}O$ ridge of Wilk-

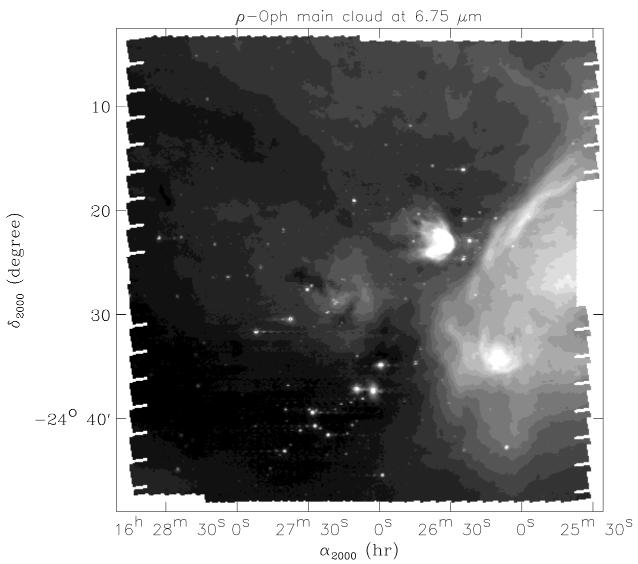

Fig. 1. ISOCAM map at 6.75 μm (for more details see the image on the ESTEC ISO WWW Server, where the emissions at 6.75 and 15 μm are coded in blue and red respectively)

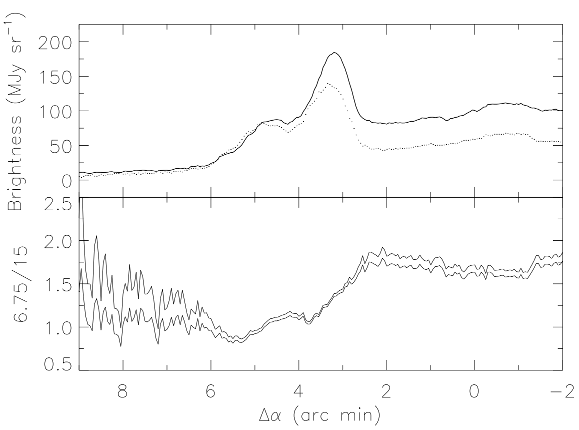

Fig. 2. Horizontal cuts across the western halo (δ_{2000}= -24° 21' 33") centered at α_{2000}=16h 25m 46.4s. Upper panel (a): 6.75 μm (solid line) and 15 μm (dotted line) emissions; Lower panel (b): $I_\nu(6.75\mu m)/I_\nu(15\mu m)$ ratio. The upper and lower curves take into account the uncertainties on the zodiacal emission correction)

ing & Lada (1983). The emission peak at $\Delta\alpha$= 3' (Fig. 2a) corresponds to these filaments and coincides with the 2 K km s^{-1} contour of $C^{18}O$ emission. The spatial coincidence between the enhanced emission and the edge of the dense ridge suggests that the filaments delineate the narrow region of interaction of the star with dense gas (the thickness of the filaments is less than 1' or 0.05 pc). They could be the fossil of dense structures in the gas not yet fully photodissociated by the UV radiation, or matter accumulated ahead of a shock (Loren & Wootten 1986) as suggested by the coherence of the polarisation angle of IR absorption in this area (Vrba at al., 1976).

One important result of the IRAS data analysis has been the disclosure of haloes of enhanced 12 μm emission relative to the 100 μm emission at the cloud edges. In the framework of the dust model of Désert et al. (1990), Bernard et al. (1993) have shown that they cannot be due to radiative transfer effects only and require a local increase of the abundance of polycyclic aromatic hydrocarbons (PAHs) and very small grains. Going from west to east, the $I_\nu(6.75\mu m)/I_\nu(15\mu m)$ color ratio across the western halo (Fig. 2b) is almost constant across the extended emission with a value 1.5–1.8, and decreases in the molecular cloud (from $\Delta\alpha$=2.5' to 3.5') to values around 1. The interpretation of these color variations and their possible relation to those seen with the $I_\nu(12\mu m)/I_\nu(100\mu m)$ ratio is not straightforward. Spectroscopic observations of one 3' field of view to the north–western corner of the image shows that features characteristic of PAHs account for ~2/3 of the integrated emission in LW2, while most of the LW3 emission comes from a continuum emission (Boulanger et al. 1996). An important information already provided by the present data is the small linear scale of < 0.05 pc over which the dust composition changes. The corresponding extinction variations are so small ($\Delta A_v \sim 0.1$ in gas at 10^3cm^{-3}) that it confirms that the color variations cannot be due to radiative transfer effects only.

Other striking features of the diffuse emission are associated to young stars. To the south-west of the image, a bow shock like structure is visible ahead of the B3 star and near IR source Elias 16 (Elias, 1978). It also coincides with the hottest ^{12}CO spot in the cloud (Encrenaz et al. 1975). The bright cometary emission around $\alpha_{2000} \sim$ 16h26m34s, $\delta_{2000} \sim$ -24°23'30", already visible on high angular resolution (30") IRAS images (Ward-Thompson 1993) is heated by an embedded B3 star which coincides with the near IR Source 1 (Grasdalen et al. 1973) (or Elias 25). This emission is resolved in the ISOCAM data into a complex network of filaments of thickness 10" or 1600 AU. To the west, the cometary emission ends at the eastern edge of the dense core Oph A (following Loren & Wootten 1986), a region of current star formation which contains the radio source VLA1623 considered as one of the youngest protostar (André et al. 1993). This coincidence suggests a close dynamical connection between the region around Source 1 and the dense core Oph A.

3.2. Deep absorption features

Deep absorptions are visible in the LW2 and LW3 maps (Fig.1) close to α_{2000}=16h27m30s, δ_{2000}=-24°27' and α_{2000}=16h28m18s, δ_{2000}=-24°19'. Since the extinction at 6.75 μm is typically 50 times lower than at visible wavelengths, this implies the existence of high column densities in compact structures. Several very dense cold regions

($n \geq 10^5 cm^{-3}$) have been detected in L1688 in HCO^+ and DCO^+ emission lines (Loren & Wootten 1986, Loren et al. 1990, herafter LWW) or in the submillimeter continuum emission (Mezger et al. 1992). The deepest absorption features (the first mentioned above) coincide with the DCO^+ and sub-mm B1 and B2 dense cores (LWW). To the first order, the IR and DCO^+ J=3-2 emissions of this region are anti-correlated which implies that the extended emission originates on the back side of the cloud.

The broad elongated ^{13}CO filament extending from Source 1 toward the North-East (Loren 1989) is also visible as a large scale absorption feature in the ISOCAM maps (Fig.1). For this reason, we believe that the whole back side of the cloud must be luminous. The Sco OB2 association, located mainly behind the cloud (de Geus et al. 1989), could be responsible for the global illumination of the far side of the cloud. This particular geometry therefore provides a unique opportunity of detecting all the opaque cores in absorption against the large scale diffuse background emission. Local heating by embedded YSOs is detectable in a few places (especially around the elbow of the B1–B2 absorption structure).

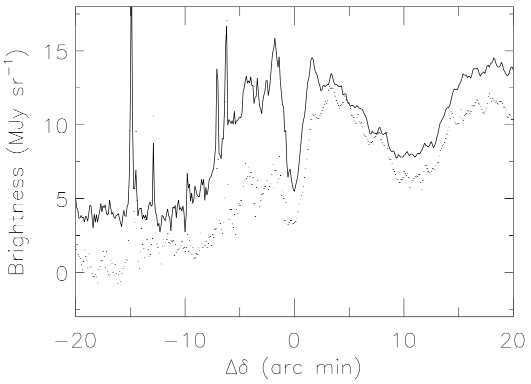

Fig. 3. Vertical cut of the whole map at α_{2000}=16h27m33s crossing the B2 dense core at δ_{2000}=-24°27', ($\Delta\delta$=0) 6.75 μm: solid line, 15 μm: dotted line.

The opacity of the B2 condensation has been estimated by interpolating the background emission between the sharp edges of the absorption profile (Fig.3). Using standard values of $\lambda\tau/N_H$ for graphite and silicate spheres (Draine & Lee 1984), we derive a central total column density of the absorbing medium N_H=1.5±0.1 $10^{23} cm^{-2}$, comparable to the value deduced from sub-mm observations (1.7-3 $10^{23} cm^{-2}$, Mezger et al. 1992).

A critical issue in the theory of star formation is the density structure of cold, dense cores in molecular clouds, likely to be the stellar progenitors. Progress there has been hampered by the limited angular resolution of millimeter continuum and molecular observations and the biases intrinsic to each density tracer. The present observations offer the possibility to map such cores with an unprecedented angular resolution. We have modeled the density structure of B2 in a cylindrical geometry to fit the observed profile: a constant density n_0 up to r=0.035 pc, and a power law decrease $n(r) \propto n_0 r^{-\beta}$ down to the density of the surrounding gas, estimated to be 10^4 cm^{-3}, according to the ^{13}CO observations of Loren (1989). The steepness of the absorption profile requires β= 3–4 and a central density n_0= 6–7 $10^5 cm^{-3}$. This structure is clearly not compatible with an isothermal self-gravitating sphere (β= 2), which has important bearings on the physics of such cores if close to hydrostatic equilibrium. Similar results have been obtained with the second absorption feature mentioned above, coinciding with the dense core Oph D (LWW). Other absorptions features are detectable in the field with a lower contrast, some of them coinciding with sub-mm emission peaks recently detected by Motte et al. (1996) or regions of bright HC_3N and CCS emission (Bernard et al. 1996).

Acknowledgements. ISO is an ESA project with instruments funded by ESA Member States and with the participation of ISAS and NASA.

References

André P., Deeney B.D., Philips R.B. et al., 1992, ApJ 401, 667
André P., Ward-Thompson D., Barsony M., 1993, ApJ 406, 122
Bernard J.P., Boulanger F., Puget J.–L, 1993, A&A 277, 609
Bernard J.P., et al., 1996, in preparation
Bertiau F.C., 1958, ApJ 128, 533
Boulanger F., Falgarone E., Puget J.–L., Helou G. 1990, ApJ 364, 136
Boulanger F., et al., 1996, this issue
Brown R.L., Zuckerman B., 1995, ApJ 202, L125
Cesarsky., C.J. et al., 1996, this issue
de Geus E.J., Zeeuw P.T., Lub J., 1989, A&A 216, 44
Désert F. X., Boulanger F.,Puget J.–L. 1990, A&A 237, 215
Draine B.T., Lee H.M., 1984, ApJ 285, 89
Elias J.H., 1978, ApJ 224, 453
Encrenaz P.J., Falgarone E., Lucas R., 1975, A&A 44, 73
Falgarone E., & Gilmore W. 1981 A&A 95 32
Grasdalen, G.L., Strom, K.M., Strom, S.E. 1973 ApJL 184 L53
Greene T.P., Young E.T., 1992, ApJ 395, 516
Loren R.B., 1989, ApJ 338, 902
Loren R.B., Wootten A., 1986, ApJ 306, 142
Loren R.B., Wootten A., Wilking B.A., 1990, ApJ 365, 269
Mezger P.G., Sievers A., Zylka R. et al., 1992, A&A 265, 743
Motte F., André P., Neri R., 1996, in preparation
Reach W.T et al. 1995. In Dwek E. (ed.) Unveiling the cosmic infrared background. AIP press, New York, p. 37
Vrba F.J., Strom S.E., Strom K.M., 1976, AJ 81, 958
Ward-Thompson D.W., 1993, MNRAS 265, 493
Wilking B.A., Lada C.J., 1983, ApJ 274, 698
Wilking B.A., Lada C.J., Young E.T. 1989, ApJ 340, 823

This article was processed by the author using Springer-Verlag LaTeX A&A style file *L-AA* version 3.